`ATOMIC-SCALE MODELING OF GRAIN BOUNDARY EFFECTS IN NANO BICRYSTAL COPPER SPECIMENS

A.M. Rajendran[1] and M.A. Zikry[2]

[1]Army Research Office, RTP, RDU, NC 27709
[2]North Carolina State University, Rayleigh, NC 27695-7910

Abstract: This paper presents results from atomistic simulations of nanobicrystal copper specimens using a Molecular Dynamics (MD) code, ParaDyn. This scalable parallel code is based on the embedded atom method (EAM). An EAM potential for copper is employed in the simulation. The main objective of the simulations was to investigate dislocation evolutions in a nanobicrystal containing a grain boundary (GB) with a certain type of misorientation. For this purpose, the MD simulations considered a Σ3 coincidence site lattice (CSL) grain boundary. Dislocation motions in nanospecimens with three different sizes under tension are evaluated from the simulations. The stress distributions, dislocation motions, and densities in the bicrystals are analyzed for a Σ3 grain boundary in straight-sided tensile specimens with the grain boundary normal to the tensile axis.

Keywords: Atomistic modeling, MD simulation, nanocrystalline Copper, dislocation motion, grain boundary, plasticity.

1. Introduction

Thermo-mechanical deformation and failure initiation and evolution in crystalline metals, alloys, and intermetallics result from various underlying mechanisms at different length scales. For instance, each grain in a polycrystalline aggregate has its distinct properties and those anisotropic properties have been studied by, for example, crystal plasticity based FEM [Kameda and Zikry 2006]. However, there could be significant differences in the atomistic behavior in the vicinity of GBs compared with the grain interiors, especially in nanocrystalline materials. Multitude of complex dislocation motions based mechanisms often dominates deformation in bulk materials as the physical scale increases from micro to mesoscale. However, at the atomistic scale, dislocation density at the interfaces increases as physical scale decreases; Dislocation mechanisms associated with high frequency of GBs, sub-grains, and cell walls may begin dominating at the interfaces. Therefore, it is important to develop a fundamental understanding of interfacial effects on dislocation kinetics in nanocrystalline metals as the physical scale decreases.

The microscopic local stress and displacement obtained by MD computation include critical information especially in GB region, and they can significantly improve the accuracy of macroscopic FEM predictions. Crystal plasticity based FEM can handle grain interior plastic deformation. In general, most crystal plasticity models do not include the effects of GB on dislocation dynamics. The continuum plasticity models tend to be "local" and the plastic deformation and damage evolution depend only on local state variables. For instance, the influence of GB misorientation, such as the Σ3 GB on the resolved effective shear stress distribution can be evaluated as a function of distance from the GB. By incorporating MD predictions into GB regions, crystal plasticity formulation can be modified to include "stress gradient" terms to track deformation behavior from dislocation nucleation to material failure. The inclusion of a stress gradient terms will thus introduce "nonlocal" characteristics into the crystal plasticity based constitutive equations. Through a hierarchical approach, the detailed evolutions of certain state variables determined from the computationally intensive MD computations for a specific GB type can be stored in a database and be used in the crystal plasticity based finite element analysis (FEA).

The mechanical characteristics of GBs vary significantly, when GB orientations vary due to distribution and orientation. With the advent of high performance computing capabilities, it is now possible to analyze large strain plasticity with MD approaches [Spearot *et al.* 2005].

Recently, Schioz [2004] performed a large scale molecular dynamic simulations of a 20-grain

nanocrystalline specimen configuration and reported a transition in the deformation mechanism at grain sizes around 10-15 nm. When the grain sizes were larger, the dislocation based plastic deformation is more or less dominated in the bulk material. The GB role or influence on the intense dislocation activity was found to be minimal. However, when the grain size was a few nanometers, the plasticity was predominantly due to grain boundary sliding. The grains were initially defects free in these simulations.

Using high resolution electron microscopy, Champion and Hÿtch [1998] showed evidence for crystallographically abrupt boundaries in nanocrystalline copper with a typical GB width of less than 0.4 nm. This measurement indicates that the GB may not play any major role in generating dislocations unless dislocations or defects are generated due to grain boundary misorientation or due to some other phenomena.

Recently, Rodney, Deby, and Verdier [2005] performed molecular static simulations of dislocations impinging on an interface between a Ni amorphous substrate and a pure Ni crystal. Their study showed formation of double interface crystal//twin/amorphous with the crystal/twin interface being a Σ3 GB. The focus was not on the dislocation dynamics related to the misorientation that present in this type of GB.

The results reported in the present study exclusively focus on the role of Σ3 GB on nucleation and propagation of dislocations in a pure Cu crystal/Cu crystal interface. One of the main objectives of this paper is to investigate GB-induced dislocations due to misorientation of grains and how these dislocations play a major role to cause plastic deformation in the bulk grain in nanocrystalline materials.

For this purpose, a nanobicrystal copper with a Σ3 GB under tensile loading conditions is considered. With the objective to determine the effects of Σ3 GB on dislocation motion and resolved shear stress, the ParaDyn simulations modeled nanobicrystal specimens of three different sizes. The effects of specimen size on dislocation nucleation, dislocation motion, and dislocation density were evaluated from a number of MD simulations.

2. Results and Discussions

To fundamentally understand and evaluate atomistic behavior of a nanobicrystal copper under tension, an embedded atom potential [Foiles *et al.* 1986] based ParaDyn MD code was employed. As shown in Figure 1, a Copper bicrystal with a Σ3 CSL orientation was chosen since Σ3 is an energetically stable GB. In CSL Σ3 contained bicrystal, the GB is the $[111]$ plane of crystal G1. The global X-axis is $[\bar{1}\,\bar{1}\,2]$ and the Z-axis is $[\bar{1}10]$. The G2 crystal is rotated 60^0 around $[111]$. This introduces a misorientation of the GB in the two crystals. A schematic of the configuration used in the ParaDyn simulation is also shown in Figure 1. The specimen dimensions are given in terms of width, depth, and length. The length of each crystal is assumed to be the same.

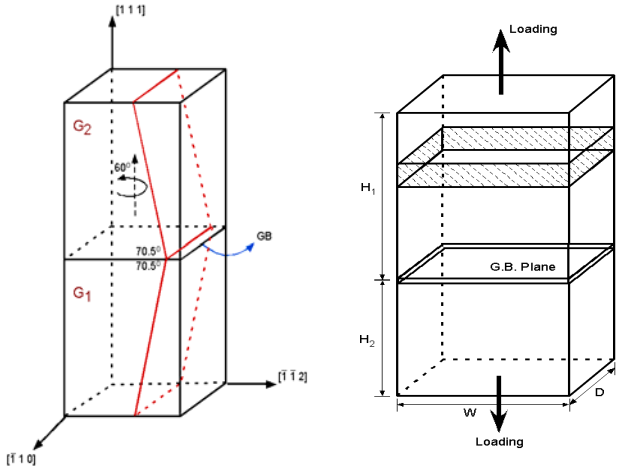

Fig 1. Schematic of the Nanospecimen

To investigate the source of defects nucleation in Σ3 GB containing crystals and to evaluate the behavior of nanocrystalline copper, three different specimen sizes, a 5 x 5 x 10, a 10 x 10 x 20, and a 20 x 20 x 40 nm are analyzed. These lengths are the total length (H1+H2) of the nanospecimen. Loading direction is normal to the GB, the boundary condition is non-periodic, the temperature was 300 K, and the applied strain rate was $10^8 s^{-1}$. To stabilize the GB region, the total potential energy is minimized by molecular statics analysis prior to the dynamic analysis. Computations are performed up to 10% nominal strain. To incorporate MD computational information, stress components and dislocation sites are obtained by specialized averaging methods. The local strains are obtained near the GB regions. The dislocation sites are

detected by a centro-symmetric parameter defined as Eqns. (1),

$$P_i = \sum_{j=1,6} \left| R_{ij} + R_{ij+6} \right|^2 \qquad (1)$$

where $\boldsymbol{R}_{ij}$ and $\boldsymbol{R}_{ij+6}$ are the bond vectors corresponding to pairs of atoms.

For the smallest specimen (5X5X10), the dislocation density ρ (1/nm^3) variation with respect to the applied nominal strain as a function of atomistic layer distance form the GB is shown in Figure 2. The atom whose centro-symmetric parameter is greater than 0.25 is also shown with a different color.

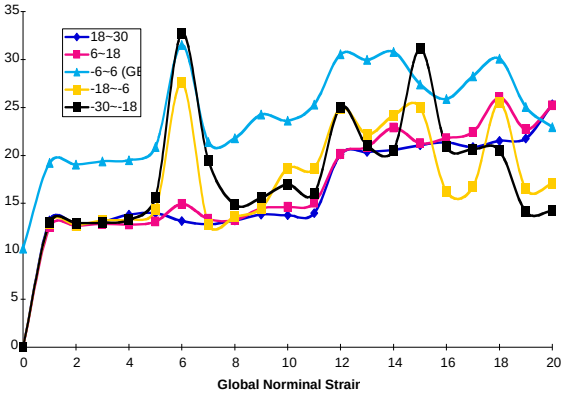

Fig. 2 Plot of Dislocation Density Vs. Strain percentage; Small specimen (5x5x20). The symbols indicate the number of layers above and below of the GB layer in crystal G1.

While the ρ jumps to about 20 nm^{-3}at less than 1% strain at the GB of the G1 crystal, the rest of the small specimen experiences a ρ of about 13 nm^{-3}. When the applied strain is increased to about 5%, new dislocations are nucleated and ρ in G1 jumps to values above 30 nm^{-3}. As the applied strain increases above 6%, the ρ in G1 relaxes to13 nm^{-3} as in rest of the specimen. However, dislocation activities continued to remain high in the GB layer. The simulations show that the dislocations are absorbed in the GB layer and not transmitted to the G2 crystal and therefore, the G2 crystal does not witness any increased dislocation activity until the strain level is increased further to above 11%. It appears that ρ continued to increase as the applied strain increases and when strains are large (>16%), the average dislocation density (ρ) in both G1 and G2 reaches values about 20 nm^{-3}. It is hard to explain or understand the microscopic mechanisms that cause the abrupt jump in ρ at 5% and 11% strains. Similarly, the unloading or annihilation of dislocations at 6% strain in the G1 crystal is unexplainable.

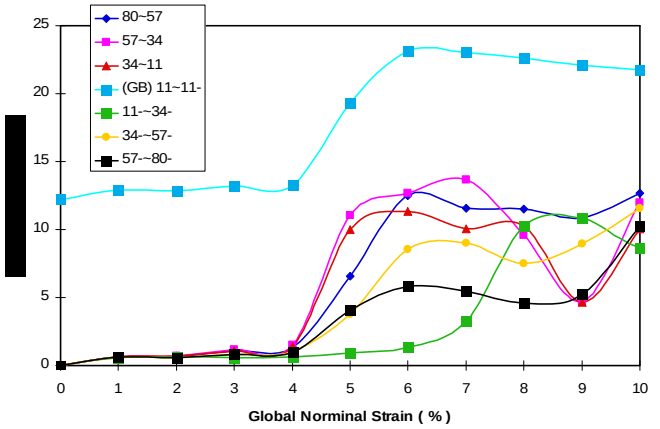

Fig. 3 Plot of Dislocation Density Vs. Strain; Large specimen (10x10x40)

The dislocation activities in the large specimen (20X20X40) were observed to be very different compared to the small specimen. Up to 4% strain, the dislocations were generated and mostly contained in the GB layer. While the ρ in GB jumped to about 20 nm^{-3} at strains < 1% in the smaller specimen (see Figure 2), it jumped to a lower value of 12 nm^{-3} in the larger specimen as shown in Figure 3. The dislocation density remained insignificant in rest of the bicrystal until 4% strain. It is interesting to notice that in the large specimen the dislocation density levels are higher in the G2 crystal than in the G1 crystal. This is completely reversed in the small specimen at least for strains less than 6%. For larger strains, ρ tend to reach an average level of 10 nm^{-3} in the bicrystal, except at the GB where it continue to remain at a higher level (~ 22 nm^{-3}).

The size effects on dislocation distributions with respect to applied strains are significant. At 10% strain, the average ρ in the small specimen is 50% more than the average value in the large specimen. The calculations were run only up to 10 % strain for the large specimen; therefore, it is not possible to compare results for strains above 10%.

Figure 4 shows a snap shot of dislocations in three different specimens at a nominal strain of 10%. The stress free boundary atoms are shown in blue color.

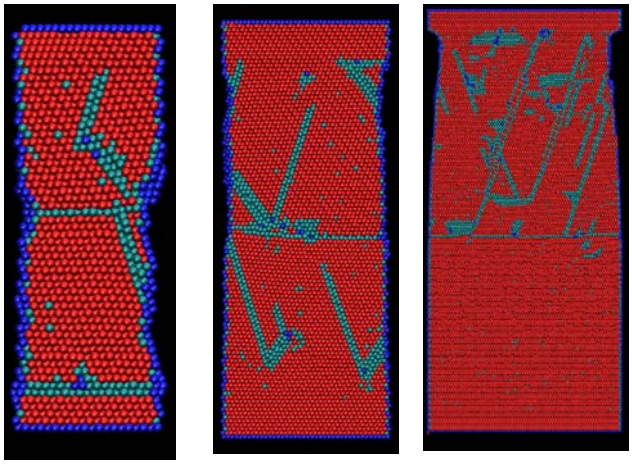

(a) (b) (c)

Fig 4. GB Dominance as Specimen Size Decreases. (a) 5x5x10; (b) 10x10x20; (c) 20x20x40

3. Summary and Recommendation

The MD simulations revealed that nucleation and propagation of dislocations in copper nano-specimens significantly varied due to specimen size and grain boundary misorientation. The grain boundary becomes the major source of dislocations generation. There seems to be a threshold strain level above which the propagation becomes more significant in all atomistic layers. The results presented in this paper are based on a limited number of MD simulations. The future research will include the effects of different grain boundaries, and boundary and loading conditions.

Acknowledgement

This work was supported by a grant of computer time from the Army's High Performance Computing Research center at University of Minnesota.

References

Champion, Y. and Hÿtch, M.J. [1998], "Evidence for Crystallographically abrupt grain boundaries in nanocrystalline copper," The European Physical Journal AP **4**, pp. 161-164.

Foiles S. M., Baskes M. I., Dow M. S., [1986], "Embedded-atom-method functions for the fcc metals Cu, Ag, Au, Ni, Pd, Pt, and their alloys", Phys. Rev. B **33**, 7983-7991.

Kameda, T., M.A. Zikry, and A.M. Rajendran, [2006] "Modeling of Grain-Boundary Effects and Intergranular and Transgranular Failure in Polycrystalline Intermetallics," *Metallurgical and Materials Transactions* A: **37A**, pp. 2107-2115.

Plimpton, S.J. and B. A. Hendrickson, [1993], "Parallel Molecular Dynamics With the Embedded Atom Method", in Materials Theory and Modelling, edited by J. Broughton, P. Bristowe, and J. Newsam, MRS Proceedings 291, Pittsburgh, PA, p. 37.

Rodney, D. J-B Deby, and M. Verdier [2005], "Atomic-scale modeling of plasticity at a metal film/amorphous substrate interface," Modeling Simul. Mater. Sci. Eng. **13**, pp.427-436.

Schiotz, Jakob [2004], "Atomic-Scale Modeling of Plastic Deformation of Nanocrystalline Copper," Scripta Materialia **51**, pp. 837-841.

Spearot D. E., Jacob K. I., McDowell D. L, *et al.*, [2005], "Effect of Deformation Path Sequence on the Behavior of Nanoscale Copper Bicrystal Interfaces", J. Engr. Materials and Technology, **127**, 374-382.